

Cochliobolus lunatus down-regulates proteome at late stage of colonization and transiently alters *StNPR1* expression in *Solanum tuberosum* L.

Bengyella Louis^{1,2,6} · Sayanika D. Waikhom^{1,6} · Robinson C. Jose¹ · Sailendra Goyari¹ · Pardeep Kumar Bhardwaj³ · Narayan C. Talukdar^{1,5} · Pranab Roy^{2,4}

Received: 7 August 2016 / Revised: 17 September 2016 / Accepted: 21 September 2016 / Published online: 30 September 2016
© Springer-Verlag Berlin Heidelberg 2016

Abstract *Cochliobolus lunatus* abundantly produces four-celled conidia at high temperatures (>30 °C) and under suitable conditions; the fungus colonizes potato (*Solanum tuberosum* L.) cultivars by adopting different invasion strategies at the microscopic level. Long-lasting defence during infection requires an upsurge in proteome changes particularly pathogenesis-related proteins chiefly under the control of nonexpresser of pathogenesis-related proteins. In order to gain molecular insights, we profiled the changes in proteome and potato nonexpresser of pathogenesis-related proteins (*StNPR1*) during the infection process. It is found

that *C. lunatus* significantly ($P < 0.05$) suppressed the host functional proteome by 96 h after infection (hai), principally, affecting the expression of ribulose biphosphate carboxylase enzyme, plastidic aldolase enzyme, alcohol dehydrogenase 2 and photosystem II protein prior to the formation of brown-to-black leaf spot disease. Strongest host response was observed at 24 hai hallmarked by 307 differentially expressed peptide spots concurring with the active phase of production of penetrating hyphae. Additionally, *C. lunatus* differentially down-regulated *StNPR1* transcript by 8.19 fold by 24 hai. This study is the first to elucidate that *C. lunatus* transiently down-regulates the expression of *StNPR1* at the onset of infection, and as a whole, infection negatively affects the expression of proteome components involved in photosynthesis, carbon fixation and light assimilation. This study contributes towards better understanding of the mechanism underlining the invasion strategies of *C. lunatus*.

Communicated by Erko Stackebrandt.

Electronic supplementary material The online version of this article (doi:10.1007/s00203-016-1297-2) contains supplementary material, which is available to authorized users.

✉ Narayan C. Talukdar
nctalukdar@yahoo.com

✉ Pranab Roy
prpranabroy94@gmail.com

¹ Institute of Bioresources and Sustainable Development (IBSD), Takyelpat, Imphal, Manipur 795001, India

² Department of Biotechnology, University of Burdwan, Golapbag More, Burdwan, West Bengal 713104, India

³ Regional Centre of the Institute of Bioresources and Sustainable Development (RCIBSD), Gangtok, Sikkim 737102, India

⁴ Department of Biotechnology, Haldia Institute of Technology, Haldia, West Bengal 721657, India

⁵ The Institute of Advanced Study in Science and Technology (IASST), Boragaon, Assam 781035, India

⁶ Department of Biomedical Sciences, School of Basic and Biomedical Sciences, University of Health and Allied Sciences (UHAS), Ho, Volta Region, Ghana

Keywords Proteome · *StNPR1* · Two-dimensional electrophoresis · qPCR · Western blotting · MALDI-TOF/TOF MS

Introduction

Cochliobolus lunatus (Nelson and Haasis) also known as *Curvularia lunata* (Wakker) Boed in recent times is known as one of the most aggressive and devastating plant pathogen causing disease in important food crops such as sorghum (*Sorghum bicolor*), wheat (*Triticum aestivum*), rice (*Oryza sativa* L), maize (*Zea mays*) and potato (*Solanum tuberosum* L.) (Agrios 2005; Iftikhar et al. 2006; Gao et al. 2012; Louis et al. 2013). Past disasters caused by *Cochliobolus* species include the Great Bengal famine where

more than 2 million people starved to death due to reduced rice yield (Scheffer 1997), corn blight epidemics in United States of America and China in 1970s and 1990s, respectively (Ullstrup 1972; Dai et al. 1995).

Morphologically, *C. lunatus* produces curved conidia, a broad rounded apex cell, a distinct swollen central cell, 4–5 distinct septa and sometimes conidia also have oval stromata (Bengyella et al. 2014). *C. lunatus* exhibits both hemibiotrophic and necrotrophic lifestyle during interaction with potato (Louis et al. 2015). During interaction with potato leaf, conidia of *C. lunatus* undergo both bipolar and unipolar germination to produce minute infection hyphae that could differentiate to appressoria-like structures, and hyphae often exhibit stomatal atropism (Louis et al. 2015). Globally, increasing pathogenic variants of *C. lunatus* and host range (Bengyella et al. 2014) have raised the curiosity among scientist to dissect *C. lunatus* proteome (Xu et al. 2007; Gao et al. 2012) and secretome (Louis et al. 2014) for pathogenicity factors. Although the proteomic studies were vital in decrypting the plethora of virulence factors, little is known on host response, as well as whether *C. lunatus* modulates the expression of nonexpresser pathogenesis-related protein 1 (herein refer as *StNPR1*, which governs the expression of pathogenesis-related proteins (PrPs)) in order to outwit systemic acquired resistance (SAR).

StNPR1 is an ankyrin repeats protein which is a key activator of PrPs that can equally activate TGA transcriptional factors to further trigger PrPs expression (Cao et al. 1997; Dong 2004; Rochon et al. 2006). Understanding how *C. lunatus* modulates the proteome and *StNPR1* in potato could allow for designing management strategies based on *StNPR1* inducers for effective priming SAR, thus, reducing crop losses from brown-to-black spot disease. Potato is produced and consumed worldwide and largely consider as “food-for-the-future” (<http://www.fao.org/newsroom/en/news/2008/1000816/>). Since it is known that *C. lunatus* adopts different strategies to invade potato cultivars at the microscopic level (Louis et al. 2015), the aim of this present study was (1) to identify important functional proteins differentially modulated during infection, and (2) to investigate whether *C. lunatus* affects *StNPR1* expression during infection. It was found that *C. lunatus* differentially suppressed potato proteome at late stages of infection and transiently down-regulated the expression of *StNPR1* during the infection process.

Materials and methods

Plant material and growth conditions

Disease-free potato (cv. Kufri Jyoti) tubers were purchased from Central Potato Research Institute (CPRI, Shimla,

India), which is *Phytophthora infestans* resistance near-isogenic lines. The tubers were grown in U-CON250 plant growth chamber (Danihan Labtech Co., Ltd) under 16 h photoperiod at the light intensity of $180 \mu\text{mol m}^{-2} \text{s}^{-1}$ and 80 % relative humidity (RH). The growth was maintained in a 90 cm × 70 cm × 12 cm capacity trays as microfield containing a mixture of autoclaved rice stalk vermicompost and sand (1:2 %w/w). Each plant was amended with 1 g organic fertilizer (BIOVITA™, PI industries Ltd, India) after 2 weeks of sprouting.

Pathogen inoculation

C. lunatus (GenBank accession JX907828) at the concentration of 10^6 conidia per ml from a 14 days old V8 agar medium plate was used. The conidial suspension was uniformly sprayed on 3-week old plants (with third fully developed terminal leaflets) using a compressed air hand sprayer till run-off. Control plants were misted with sterile water only. The experimental set-up was maintained at 20 °C and 100 % RH in the growth chamber. Infectivity of the plants was confirmed microscopically using a microscope coupled with DP7M5.0.0.5 software and an Olympus DP70 camera (Olympus BX61®, USA). The experiment was performed in replicate and repeated three times.

Protein extraction and quantification

Leaf samples were randomly collected by 24, 48, 72 and 96 h after inoculation (hai) for challenged and control plants at the same time point. One gram sample was immediately flash frozen in liquid nitrogen and crushed into fine powder. The proteins were extracted on ice in a 9 mM CaCl_2 solution (containing 5 %v/v Triton-X-100, 0.2 % w/v polyvinylpyrrolidone and 0.2 %w/v dithiothreitol (DTT), 0.2 % L-ascorbic acid), pH 4.8 as earlier described (Waikhom et al. 2015). Proteins from three biological repeats were pooled and washed using Clean-Up Kit (Bio-Rad® laboratories, CA, USA) following the manufacturer protocol. For all downstream analysis, proteins were quantified using the Bradford dye-binding assay (Bio-Rad, CA, USA).

Expression of *StNPR1* by Western blotting

Thirty-five microgram samples were profiled by SDS-PAGE (5–13 % polyacrylamide gel, Sigma) and transferred to a PVDF membrane with a Trans-Blot® Turbo™ transfer system (Bio-Rad®, CA, USA). Membranes were incubated with 1:10,000 diluted *Arabidopsis thaliana* (AtNPR1) primary antibody (kindly provided by Prof. Xiannian Dong, Duke University, USA) overnight at 4 °C. After a series of washing, blots were further incubated with 1:50,000

diluted HRP-conjugated secondary antibody (Bio-Rad®, CA, USA) for 1 h at room temperature. The signals were detected by chemiluminescent kit and imaged in Chemi-Doc XRS (Bio-Rad®, CA, USA). The densitometry analysis was performed and may not certainly reflect the expression threshold of target protein signal and statistically analysed in R tool using one-way Anova test for the levels of significance.

Two-dimensional gel electrophoresis for proteome profiling

Cleaned proteins were suspended in ReadyPrep rehydration buffer (containing 8 M urea, 50 mM DTT, 2 % 3-[(3-cholamidopropyl)dimethylamino]-1-propanesulphonate, 0.2 % (w/v) Biolyte® 3/10 ampholytes, and bromophenol blue trace; Bio-Rad®, CA, USA) and quantified by the dye-binding method. Isoelectric focusing (IEF) was performed in Protean®i12™ IEF CELL apparatus (Bio-Rad®, CA, USA). After preliminary testing of the immobilized pH gradient (IPG) strips of different pH ranges, we found that only pH 4–7 produced the best resolution. A 7 cm IPG dry strips with a linear pH range of 4–7 was rehydrated passively with 180 µg protein aliquots for 16 h and run as previous described (Louis et al. 2014). Following IEF, IPG strips were equilibrated for 45 min at room temperature with equilibration buffer I (6 M urea, 2 % SDS, 0.375 M Tris–HCl pH 8.8, 20 % glycerol and 56 mM dithiothreitol (DTT)), and then transferred to equilibration buffer II (6 M urea, 2 % SDS, 0.375 M Tris–HCl pH 8.8, 20 % glycerol and 3.5 mM DTT). In the second dimension, that is 1-D, the proteins were resolved on 15 % polyacrylamide ultrathin gels (7.3 cm × 8 cm × 0.75 mm) at 80 V using Mini-Protean®TetraCell (Bio-Rad®, CA, USA). All gels were stained with 0.35 % w/v extrapure Coomassie Brilliant-blue R250 at 38 °C overnight. Gels were destained in a solution containing 7 % acetic acid and 35 % methanol till spots were visible, imaged and repeated three times per sample.

Identification of the host metabolic pathway significantly affected by infection

To determine whether the infection process alters the host proteome, images were processed in Progenesis SameSpot 4.1 (Total-Lab, USA) as follows. Following quality control of 2-D gels, only spots with pixel-to-pixel intensity ≥ 120 matching each other in three independent gels per sample were normalized and spots counts were performed. To have an in-depth view in variations in proteome, generated data were analysed in QluCoreOmics Explorer 2.3 software. Two group comparison (t-test) was applied for heatmap hierarchical clustering at $t_{141} \leq 1.347$, $R \leq 0.113$, $q = 0.450$,

$p = 0.91$ and filter by variance ($\sigma/\sigma_{\max} = 0.053$) cut-off value for control and challenge proteome at 96 hai. To identify which component of the host metabolic pathway was the most affected by the infection process, spots with fold expression (FE) ≥ 3.0 at Anova value $P < 0.05$, and judged to significantly vary at 24, 48, 72 and 96 hai compared to control were sorted, excised and submitted for identification.

Peptide spots were trypsinized and protein elution was performed as earlier described (Shevchenko et al. 2006) and peptide solution was concentrated in a vacuum centrifuge to approximately 10 µl volume. Four microlitre of trypsinized peptide solution was mixed with α -cyano-4-hydroxycinnamic on target plate of matrix-assisted laser desorption/ionization time-of-flight/time-of-flight mass spectrometry (MALDI-TOF/TOF MS) and allow to crystallize at room temperature. The analysis was performed in a MALDI-TOF 4800 proteomics analyser (Applied Biosystem, MDS SCIEX4800, USA). The study was performed in a positive reflectron mode at 25 kV, 50 ns delayed extraction time and mass spectra were acquired in the default mode and generated data were processed using DataExplorer 5.1 (Applied Biosystems®, USA). Spectra peak lists obtained were processed through in-house MASCOT search engine (v.2.3 Matrix Science, London, UK) against all new entries in the green plant MSDB, NCBI nr databases and mapped to phytozome 11 (*S. tuberosum* v3.4 genome). Search parameters were: trypsin as enzyme, variable modifications like carbamidomethyl, fixed modification for cysteine residues, up to one cleavage, error tolerance of ± 100 ppm, ± 0.2 Da, oxidation of methionine and N-terminal acetylation were taken into consideration. At a MOWSE probability threshold score ($P < 0.05$) peptide were considered, and false-discovery rate (FDR; Elias et al. 2005) was calculated using Decoy database (http://www.matrixscience.com/help/decoy_help.html) and validated at FDR < 1 %.

Gene expression analysis during infection

RNA was isolated by using TRI reagent kit according to the manufacturer's instructions (Sigma, St. Louis, MO, USA). The quality and quantity of RNA were evaluated using a 1 % agarose gel and nanoDrop spectrophotometer (Bio-SpecNanodrop™, Shimadzu), respectively. cDNA was synthesized with Invitrogen kit according to the manufacturer instructions (Invitrogen™ Life Science Software, Invitrogen Inc.), and the quality and integrity of cDNA were verified by performing PCR with 26S rRNA using the primer set 26S-F: 5'-cacaatgataggaagaccgac-3' and 26S-R: 5'-caagggaacgggcttgccagaatc-3' (Fig. S3). Real-time quantitative polymerase chain reaction (RT-qPCR) was performed using the iScript™ One-Step RT-PCR Kit with 2X SYBR® Green buffer (Bio-Rad, USA) containing 0.4 mM of dNTP [of dATP, dCTP, dGTP, dTTP], magnesium chloride, iTaq

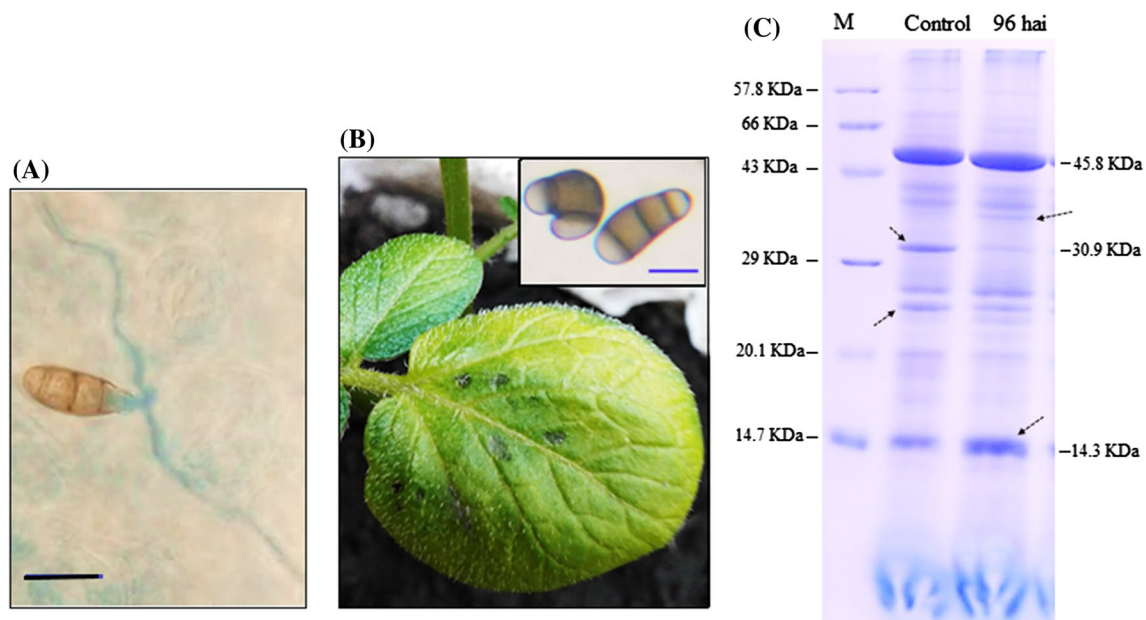


Fig. 1 **a** Invasion of potato leaf by *C. lunatus* at 12 hai stained with trypan-blue-chlorazol black E-KOH as previously described (Louis et al. 2015) and observed with a bright-field Olympus BX61 microscope coupled with DP7M5.0.0.5 software. **b** Brown-to-black spot disease of potato at 96 hai and the close-up represents micrograph

of *C. lunatus* at resting state. **c** Crude protein (35 μ g) extracted from potato leaf cv. Kufri Jyoti, lanes from left to right, molecular weight markers, control plants mist with sterile water and plants challenged with *C. lunatus* for 96 h. The broken arrows indicated prominent differentially expressed peptides bands

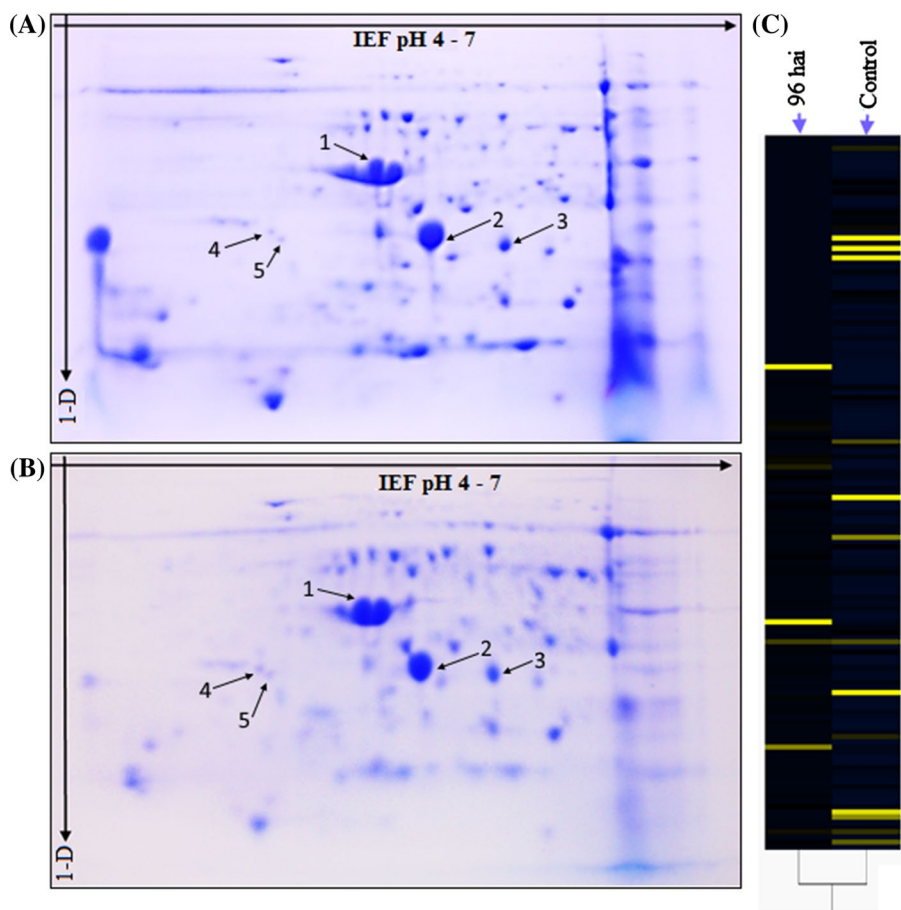
DNA polymerase, 20 nM fluorescein, SYBR[®] Green I dye), stabilizers nuclease-free H₂O, 10 fold diluted total cDNA, 0.3 μ L of 10 μ M of each primer—*StNPR1*-F: 5'-gctgaaatgctcagggtga-3', *StNPR1*-R: 5'-cagcgtaatgaagcgtga-3' (product size 145 bp based on GenBank accession AY615281). Amplification conditions were as follows: 95 °C for 10 min, followed by 40 cycles of 95 °C for 10 s, 54 °C for 30 s and 72 °C for 30 s. The potato β -tubulin gene Z33382 was included as internal positive control using the primer set Tu-F: 5'-tctgcaacctgagtggtgt-3' and Tu-R: 5'-atgttgctctcgcttcagt-3'. Negative controls (without cDNA templates) containing primers were run to check the absence of primer dimers and contamination. Also, primers (Table S1) representing genes encoding for the peptide spots that were significantly affected (at FE \geq 3) at 24, 48, 72, and 96 hai during the infection process were validated by RT-qPCR. The primers were designed using OligoPerfect[™] Designer software (Invitrogen[™] Life Science Software, Invitrogen Inc.). The amplification kinetics was determined as mean of three independent experiments. The relative gene expression was computed using fold induction equation = $2^{-\Delta\Delta C_t}$ as previously described (Trouvelot et al. 2008). The experiment was performed in StepOne[™], StepOnePlus[™] Real-Time PCR Systems (Applied Biosystem[®], Life Technologies) and all data subjected to *t* test for the level of significance.

Results and discussion

lunatus suppresses host proteome during infection

A key area for understanding the mechanism employed to overcome potato defence is to study the changes in functional proteome since vital information on host physiological process could be derived. *C. lunatus* is a rapid colonizer of potato and by 24 h after inoculation (hai), we confirmed pathogenic relationship was established (Fig. 1a). As previously shown (Louis et al. 2015), the development of brown-to-black spots disease was hallmarked by minute colonizing hyphae from germinated conidia (Fig. 1a, b). Symptoms of *C. lunatus* infection in potato leaf consist of yellowing of leaf, water-soaked brown-to-black spots (Fig. 1b) and wilting at the advanced stage of infection. To gain insights whether *C. lunatus* invasion influences the host response at the proteome level, protein samples collected at 96 hai and control plant were comparatively profiled. Prominently, we found that by 96 hai, proteins within 30.91 kDa limit were suppressed, whereas proteins within 14.31 kDa were either over-expressed or induced (Fig. 1c). This result showed that *C. lunatus* modified host proteome during the infection process and warranted in-depth investigation into the functional proteins most affected during infection.

Fig. 2 **a** 2-D map for control potato leaf proteome with 213 spots, **b** 2-D map for potato plants challenged for 96 hai with 97 spots. **c** Heatmap was generated in QlucoreOmics Explorer 2.3 depicting hierarchical clustering of proteome changes between control and challenged plants based on normalized relative spots volume ($P < 0.05$). Each line corresponds to a spot and unique spots with fold expression >2.5 are conspicuously represented



Two-dimensional gel electrophoresis (2-D) was performed to unravel the extent in protein alteration during the colonization process. Proteome maps at 24, 48, 72 and 96 hai were generated and compared against controls at the same time point. As observed using one-dimension gel electrophoresis (Fig. 1c), 2-D map revealed 97 spots in *C. lunatus*-challenged plants at 96 hai against 143 spots in control plants confirming an overall down-regulation in protein expression during infection at that time point (Fig. 2). Furthermore, mean changes in the number of peptide spots were as follows, 24 hai (307 spots, Fig. S1), 48 hai (274 spots, Fig. 3), 72 hai (269 spots, Fig. S2). These spots were reproducibly observed in 2-D independently run experiments. This analysis reinforces the evidence that *C. lunatus* suppressed potato leaf proteome during infection.

In order to determine the most prominent component of the proteome affected by *C. lunatus* infection, 2-D profiles were compared in Progenesis SameSpot 4.1 suite and peptide spots with mean fold expression at all time points ≥ 3 at Anova $P < 0.05$ were sort out and tagged (Figs. 2, 3, S1, S2). The expression profiles of the tagged spots are provided (Fig. 4a), and their identity following MALDI-TOF/TOF MS is shown (Table 1). Peptide spot# 1 was identified as ribulose biphosphate carboxylase enzyme (EC 4.1.1.39;

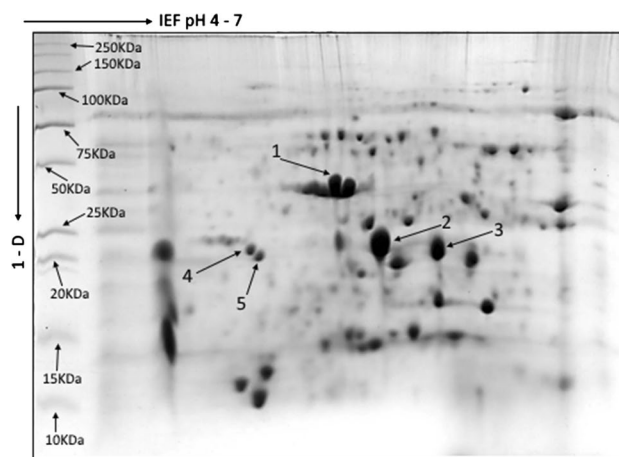


Fig. 3 2-D proteome map of potato leaves at 48 hai of *C. lunatus*. Spots of interest with fold expression >3 are indicated with arrows. The immobilized pH gradient scale and Precision Plus Protein™ WesternC™ Standards are shown

RUBISCO) which catalyses the rate determining step of photosynthesis and was down-regulated at the onset of the infection process (Fig. 4a), nonetheless, up-regulated at 96 hai. Peptide spot# 2 was identified as plastidic aldolase

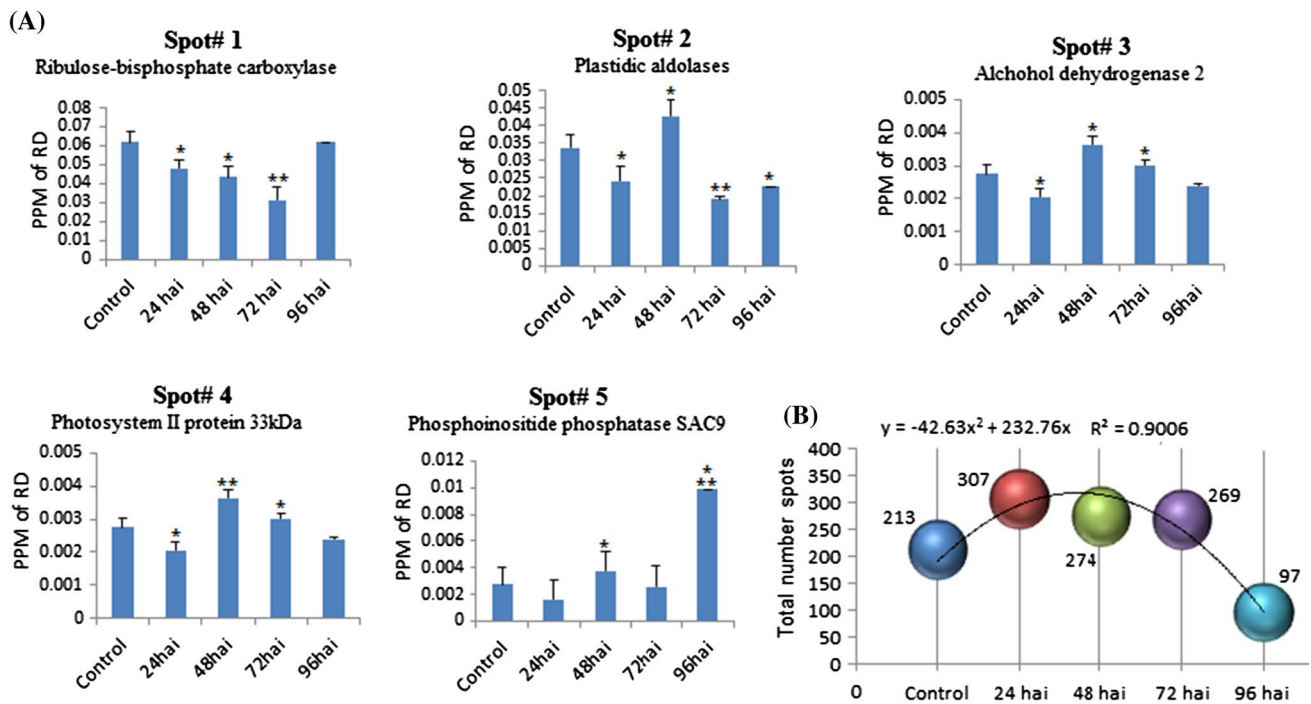


Fig. 4 **a** View of differentially expressed peptide spots significantly and severely affected during infection in part per million (PPM) of relative density (RD). The graph represents mean of three biological replicates and bars are mean standard error, and asterisk

indicates the level of significance. **b** A global view for mean peptide spots in potato leaf proteome during *C. lunatus* infection. Asterisks indicate levels of significant differences in expressed peptide spots (* $P < 0.05$; ** $P < 0.01$; *** $P < 0.001$)

enzyme which catalyses the formation of triose phosphate, and whose expression was high at 48 hai. Peptide spot# 3 was identified as alcohol dehydrogenase 2 which catalyses the interconversion of aldehydes, ketones and alcohols and was differentially expressed at all time points. Peptide spot# 4 was identified as photosystem II protein, a light harvesting protein, whose expression level was high at 48 hai. Considering spot# 3 and 4 expression levels decreased steadily as from 48 hai (Fig. 4a), it is not unreasonable to propose that carbohydrate metabolism is severely affected during infection. Previously, attempt to unravel maize resistance to *C. lunata* using proteomics approach led to cataloguing of 100 differentially expressed spots, and identification of eight selected spots, among which two oxygen-evolving enhancer proteins were identified (Huang et al. 2009; Pechanova and Pechan 2015), akin to photosystem II protein identified herein (spot# 4). Other studies have suggested that photosystem II proteins are responsive to biotic and abiotic stresses (Sugihara et al. 2000; Wu et al. 2013). Peptide spot# 5 was identified as phosphoinositide phosphatase SAC9, whose expression was steadily up-regulated (Fig. 4a). Phosphoinositide phosphatase SAC9 is involved in modulating phosphoinositide signalling pathways during stress response (Williams et al. 2005). Overall, the strongest host response following *C. lunatus* infection was observed at 24 hai hall-marked by 307 peptide spots (Fig. 4b).

From this study, *C. lunatus* infection negatively impacts on the energy pathway, that is, disrupt the potential to harness light energy during photosynthesis (spot#1 and 4) and alters carbohydrate catabolic pathway (spot# 3). Thus, this interference could deprive the host of vital energy and could explain drying and wilting observed at advance stages of infection. Given that *C. lunatus* produces diverse conidia (Louis et al. 2015), significant quantity of melanin and nonhost specific toxin such as methyl-5-hydroxymethylfuran-2-carboxylate (Goa et al. 2014) that could aid in niche exploitation and host pathogenicity, it would be interesting to investigate the effects of these metabolites on RUBISCO, alcohol dehydrogenase 2, plastidic aldolase and photosystem II protein 33 kDa. To validate the expression of peptide spots at the mRNA level, RT-qPCR was performed and found to be differentially expressed at all time point similar to peptide spots (Fig. 5).

C. lunatus transiently suppressed the expression of *StNPRI* at the onset of infection

The expression kinetics for *StNPRI* expression was determined by RT-qPCR and by 24 hai, *C. lunatus* infection significantly down-regulated *StNPRI* by 8.19 fold below the constitutive level in control plant (Fig. 6a). By 48 hai and 72 hai, *StNPRI* transcript decrease below the basal

Table 1 Details of identified proteins by MALDI-TOF-MS analysis with significant differential expression kinetics during invasion of potato by *Cochliobolus lunatus*

Spot no.	Source in MSDB and NCBInr	Protein name	NCBInr accession	Hit in <i>S. tuberosum</i> v3.4 genome, phytozome 11	Physiological role	PS/PV/pI/Mwt	Differential expression at different time point in hai			
							24	48	72	96
1	<i>S. tuberosum</i> L.	Ribulose biphosphate carboxylase (EC 4.1.1.39)	gi 21567	PGSC0003DMG400012666	Anabolism, catalyses atmospheric CO ₂ fixation in plants	107/99/7.04/20.30	↓	↓	↓	↑
2	<i>S. tuberosum</i> L.	Plastidic aldolases	gi 1781348	PGSC0003DMG400003123	Catabolism, cleavage of aldol into triose phosphates molecules	46/68.2/5.74/38.48	↓	↑	↓	↑
3	<i>S. tuberosum</i> L.	Alcohol dehydrogenase 2	gi 13958655	PGSC0003DMG400030771	Catabolism/anabolism, of aldehydes, ketone and alcohols	33/46.8/5.66/41.11	↓	↑	↑	↓
4	<i>S. tuberosum</i> L.	Photosystem II protein 33 kDa	gi 19157	PGSC0003DMG400002782	Anabolism, a light harvesting protein	127/53.7/5.81/34.96	↓	↑	↓	↓
5	<i>S. tuberosum</i> L.	Probable phosphoinositide phosphatase SAC9	gi 565362612	PGSC0003DMG400028855	Interaction module in diverse set of signalling proteins	54/90.2/5.57/78.37	↓	↑	↓	↑

Ps/Cov—protein score/amino acid coverage reported by MASCOT MS Ion search at MOWSE probability threshold score $P < 0.05$; pI/Mwt—theoretical isoelectric pH and molecular weight in kDa. NM—number of matches; PTM—post-translational modifications at the N-terminal sequence. Arrows pointing up and down represent up-regulated and down-regulated peptide spots, respectively

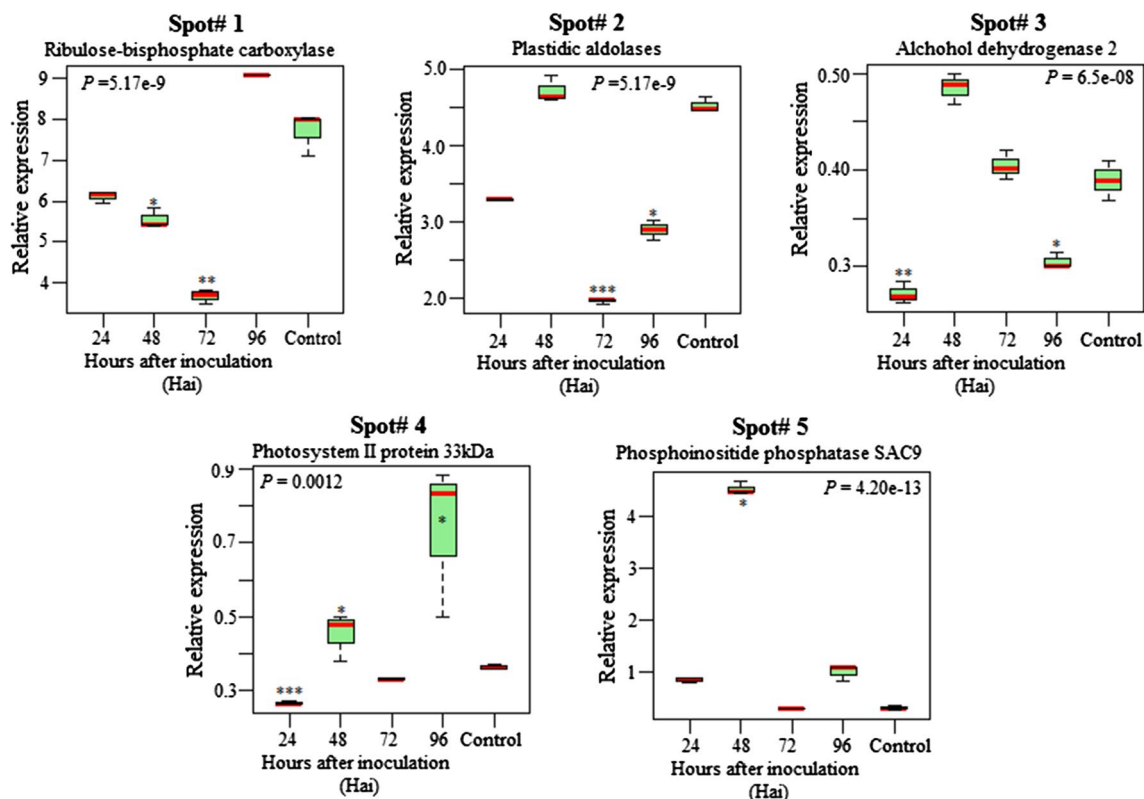
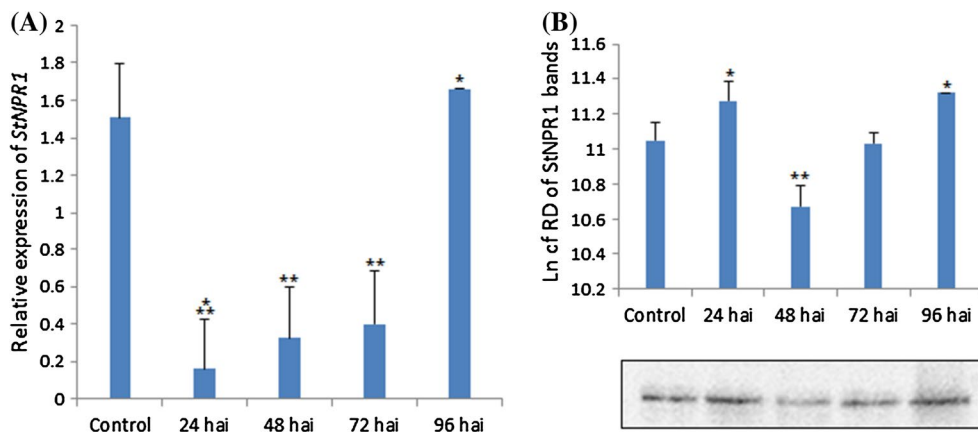


Fig. 5 Boxplots illustrate the relative mRNA expressions level for corresponding peptide spots# 1, 2, 3, 4 and 5 affected during *C. lunatus* infection. The differences between groups were computed,

error bars refer to standard deviation between replicates and *asterisk* indicates the level of significance with respect to control (* $P < 0.05$; ** $P < 0.01$; *** $P < 0.001$)

Fig. 6 a Expression profile of *StNPR1* as determine by real-time quantitative PCR. **b** Western blot analysis depicting the expression of *StNPR1* in potato leaf at different time points expressed as mean of relative density. The values represent mean values and *bars* are standard error of mean values and *asterisk* indicates the level of significance (* $P < 0.05$; ** $P < 0.01$; *** $P < 0.001$)



expression level. It was observed that at 96 hai *StNPR1* transcript level increased by 1.03 fold above the constitutive threshold level.

Western blot analysis showed *StNPR1* expression decreases at 48 hai prior to an upsurge in *StNPR1* level as from 72 hai (Fig. 6b). Despite the increase in *StNPR1* levels by 96 hai as revealed by blotting and RT-qPCR, the overall proteome change decreased (Fig. 4b) at the same time point, indicating that *C. lunatus* suppressed potato leaf

proteome during the formation of brown-to-black spot disease. From this result (Figs. 4b, 6b), there is no direct correlation between the overall proteome change and *StNPR1* expression. By comparing *StNPR1* transcript and *StNPR1* protein levels (Fig. 6), an increasing trend was observed except at 24 hai where *StNPR1* protein level was high and *StNPR1* transcript was low. Studies have shown that strict correlation between mRNA–protein abundance in the cell is rare and often poor (Maier et al. 2009). Herein, the

discrepancies could be associated with hyper-accumulation of *StNPR1* when the colonization process is heightened at 24 hai (Fig. 1a) and host response is highest, hallmarked by an overall high number of peptide spots (Fig. 4b). Thus, it is not unreasonable to observe the low level of *StNPR1* at 24 hai, but we propose that once mRNAs are translated following post-translational modifications, *StNPR1* accumulates despite the low mRNA levels. Being a regulatory protein, *StNPR1* is then progressively turned-over as from 48 hai when the host defence is progressively subdued. The makeover of local infection into global defence (or SAR) largely depends on the expression of *StNPR1*. A pathogen capable of transiently down-regulating *StNPR1*, such as *C. lunatus*, could rapidly restrains the fine-tuning process which leads to massive transcriptional and proteome reprogramming to turn local infection into SAR, rendering the host vulnerable to irreversible colonization.

Conclusion

Infection strategies of potato by *C. lunatus* include formation of appressoria-like structure to penetrate different potato genotypes, secretion of diverse effectors and metabolites, modulation of ambient microenvironment, virulence differentiation and induce-virulence variations on maize crop. *C. lunatus* represents a formidable challenge in agriculture because of its ability to modulate host defences and expand its host range. In this study, it is shown that the brown-to-black spot disease caused by *C. lunatus* is associated with suppression of proteome and transient down-regulation of *StNPR1* transcript at the onset of colonization. Also, this study shows that *C. lunatus* chiefly mitigates protein components involved in photosynthesis, carbon fixation and light assimilation.

Acknowledgments This research was jointly supported by The World Academy of Sciences (TWAS), Trieste, Italy and the Department of Biotechnology, Government of India (DBT/TWAS PG fellowship No. 3240223450) and Alexander von Humboldt (AvH) foundation. The authors thank DK Hore for proofreading the manuscript.

References

- Agrios GN (2005) Plant pathology, 5th edn. Academic Press, Amsterdam, p 395p
- Bengyella L, Waikhom SD, Roy P, Bhardwaj PK, Sharma CK, Singh MW, Talukdar NC (2014) Host-range dynamics of *Cochliobolus lunatus*: from a biocontrol agent to a severe environmental threat. *BioMed Res Int*, Article ID 378372, p 9. Doi: 10.1155/2014/378372
- Cao H, Glazebrook J, Clarke JD, Volko S, Dong X (1997) The *Arabidopsis NPR1* gene that controls systemic acquired resistance encodes a novel protein containing ankyrin repeats. *Cell* 88:57–63
- Dai FC, Gao WD, Wu RJ, Jin XH (1995) A noticeable corn disease: *Curvularia* leaf spot. *Acta Phytopathol Sin* 25:330
- Dong X (2004) NPR1, all things considered. *Curr Opin Plant Biol* 7:547–552
- Elias JE, Haas W, Faherty BK, Gygi SP (2005) Comparative evaluation of mass spectrometry platforms used in large-scale proteomics investigations. *Nat Methods* 2:667–675
- Gao S, Liu T, Li Y, Wu Q, Fu K, Chen J (2012) Understanding resistant germplasm induced virulence variation through analysis of proteomics and suppression subtractive hybridisation in a maize pathogen *Curvularia lunata*. *Proteomics* 12:3524–3535
- Goa J-X, Liu T, Chen J (2014) Insertional mutagenesis and cloning of the gene required for the biosynthesis of the non-host specific toxin in *Cochliobolus lunatus* that causes maize leaf spot. *Phytopathology* 104:332–339
- Huang X, Liu L, Zhai Y, Liu T, Chen C (2009) Proteomic comparison of four maize inbred lines with different levels of resistance to *Curvularia lunata* (wakter) boed infection. *Prog Nat Sci* 19:353–358
- Iftikhar A, Shazia I, Cullum J (2006) Genetic variability and aggressiveness in *Curvularia lunata* associated with rice-wheat cropping areas of Pakistan. *Pak J Bot* 38(2):475–485
- Louis B, Roy P, Waikhom SD, Talukdar NC (2013) Report of foliar necrosis of potato caused by *Cochliobolus lunatus* in India. *Afr J Biotechnol* 12:833–835
- Louis B, Waikhom SD, Roy P, Bhardwaj PK, Singh MW, Goyari S, Sharma CK, Talukdar NC (2014) Secretome weaponries of *Cochliobolus lunatus* interacting with potato leaf at different temperature regimes reveal a CL[xxxx]LHM-motif. *BMC Genom* 15:213
- Louis B, Waikhom SD, Jose RC, Goyari S, Talukdar NC, Roy P (2015) *Cochliobolus lunatus* colonizes potato by adopting different invasion strategies on cultivars: new insights on temperature-dependent virulence. *Microb Pathog* 87(2015):30–39
- Maier T, Güell M, Serrano L (2009) Correlation of mRNA and protein in complex biological samples. *FEBS Lett* 583(24):3966–3973
- Pechanova O, Pechan T (2015) Maize-pathogen interactions: an ongoing combat from a proteomics perspective. *Int J Mol Sci* 16:28429–28448
- Rochon A, Boyle P, Wignes T, Fobert PR, Despres C (2006) The co-activator function of Arabidopsis NPR1 requires the core of its BTB/POZ domain and the oxidation of C-terminal cysteines. *Plant Cell* 18:3670–3685
- Scheffer RP (1997) The nature of disease in plants. University Press, Cambridge
- Shevchenko A, Tomas H, Havlis J, Olsen JV, Mann M (2006) In-gel digestion for mass spectrometric characterization of proteins and proteomes. *Nat Protoc* 1:2856–2860
- Sugihara K, Hanagata N, Dubinsky Z, Baba S, Karube I (2000) Molecular characterization of cDNA encoding oxygen evolving enhancer protein 1 increased by salt treatment in the mangrove *Bruguiera gymnorhiza*. *Plant Cell Physiol* 41:1279–1285
- Trouvelot S, Varnier AL, Allergre M, Mercier L, Baillieuil F et al (2008) A beta-1, 3 glucan sulphate induces resistance in grapevine against *Plasmopara viticola* through priming of defense responses, including HR-Like cell death. *Mol Plant Microbe Interact* 21:232–243
- Ullstrup AJ (1972) The impact of the southern corn leaf blight epidemics of 1970–71. *Annu Rev Phytopathol* 10:37–50
- Waikhom SD, Louis B, Pranab R, Talukdar NC (2015) Insights on predominant edible bamboo shoot proteins. *Afr J Biotechnol* 14(17):1511–1518
- Williams ME, Torabinejad J, Cohik E, Parker K, Drake EJ, Thompson JE, Hortter M, Dewald DB (2005) Mutations in the *Arabidopsis* phosphoinositide phosphatase gene SAC9 lead to over-accumulation of ptdIns(4,5)P2 and constitutive expression of the stress-response pathway. *Plant Physiol* 138:686–700

- Wu L, Han Z, Wang S, Wang X, Sun A, Zu X, Chen Y (2013) Comparative proteomic analysis of the plant-virus interaction in resistant and susceptible ecotypes of maize infected with sugarcane mosaic virus. *J Proteome* 89:124–140
- Xu S, Chen J, Liu L, Wang X, Huang X, Zhai Y (2007) Proteomics associated with virulence differentiation of *Curvularia lunata* in maize in China. *J Integr Plant Biol* 49(2007):487–496